

Figure 94. **Reprocessed MT-104-9**, pod #s 4, 5 and 8 treated with Sypro[®] Orange protein stain. Projections (maximum intensity method) of series of optical sections collected from the laser scanning confocal microscope through the hypotube area of the pod following treatment with 2 μ M of the stain Sypro[®] Orange. Bright regions indicate positive staining for protein. The unstained control image through the same area of the hypotube as the other images is in figure 84.

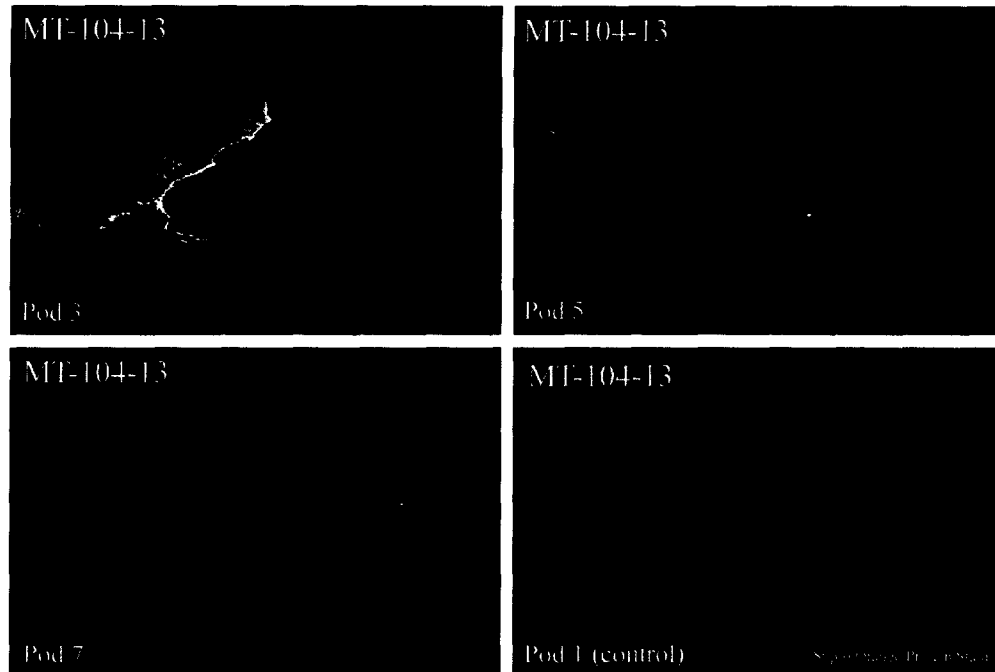


Figure 95. **Reprocessed MT-104-13**, pod #s 3, 5 and 7 treated with Sypro[®] Orange protein stain. Projections (maximum intensity method) of series of optical sections collected from the laser scanning confocal microscope through the hypotube area of the pod following treatment with 2 μ M of the stain Sypro[®] Orange. Bright regions indicate positive staining for protein. Pod #1 is an unstained control image through the same area of the hypotube as the other images. The control image shows a low level of autofluorescence.

Table II.
Summary of reprocessed Octopus devices stained for DNA and Protein

Device code ID	Pod # Control	Pod # PI or Syto 16 Nucleic Acid Stain	Pod # Sypro [®] Orange Protein Stain
MT-104-1	5	1 3 5 7	
MT-104-2	2	2 4 6 8	
MT-104-3	5	2 5 6	
MT-104-4	1	2* 4 6 8	
MT-104-5	1	2* 4 6 8	3 5 7
MT-104-8	1	2 4 6 8	3 5 7
MT-104-9	3	1 2 5 6	4 5 8
MT-104-10	5	3 4 7 8	
MT-104-11	7	1 2 6 8	
MT-104-13	1	2 4 6 8	3 5 7
MT-104-16	8	3 4 6 7	

* Note: MT-104-3 MT-104-5 and 7 pod #2 was observed using DAPI stain as well. MT-104-7 was not included in the DNA/protein staining because it was selected to be cut apart to expose the hypotube interior.

DNA Analysis

Following initial imaging and prior to disassembly and cutting of the tubes, samples of content from designated pods (see Table III) of the new and reprocessed Octopus 3[®] and Octopus 4[®] devices were collected using sterile swabs. DNA was identified using a Quiagen DNeasy tissue kit (cat # 69502 Quiagen, Valencia, CA) as per kit instructions. Briefly, following swabbing of an individual pod, the swab end was treated with proteinase K at 70°C for 1 hour to lyse cellular material. 200 μ l of Buffer AL was added and sample vortexed. 200 μ l of EtOH was added and vortexed. The entire sample was placed into DNeasy mini spin column and spun at 6000g for 1 minute. The collection tube was discarded. 500 μ l of Buffer AW1 was added and spun at 6000g for 1 minute. The flow-through and tube was discarded. 500 μ l of Buffer AW2 was added and spun at 20,000 x g for 3 minutes. The column was washed 2 times with 200 μ l of Buffer AE, incubated for 1 minute and spun at 6000 x g for 1 minute.

A single-copy 536 bp human β -globin fragment was amplified from each sample using standard PCR protocols, and the products electrophoresed on a 10% polyacrlamide/TBE gel and stained with ethidium bromide (Molecular Probes). Gels were photographed using a BioDocIt gel documentation system (UVP Inc.).

Briefly, PCR was preformed by using one hundred picograms of DNA in quadruplicate 20 μ l parallel PCR assays using a Perkin Elmer 9700 thermal cycler. The fluorescence of 0.25x SYBR-Green (Molecular Probes, Eugene, OR) was measured at each amplification step. Sixty cycles of PCR were carried out using the HotStar *Taq* polymerase system (Qiagen, Valencia, CA) with the primer pairs below at the specified annealing temperatures.

Primer: TTT AGT GGG GTA GTT ACT CCT

Product length 540, $T_a=60.4$, Read Temp=77.5

This primer is designed to amplify the genes corresponding to β -globin region of human genome DNA. This primer is used as the positive control for confirming the presence and the acceptability of the extracted DNA to template. PCR and gel electrophoresis performed by external staff.

Due to unknown prior treatments of reprocessing and the small amount of sample material collected it is likely that the DNA positive results may be under represented.

Table III.
Summary of reprocessed Octopus devices analyzed for human β -globin fragment by PCR

Device code ID	Pod # Analyzed	Result
MT-104-1	1 3 5 7	
MT-104-2	4, 8	
MT-104-3	1 3 5 7	Positive 5, 7
MT-104-4	4, 8	
MT-104-5	4, 8	
MT-104-7	2, 7	Positive 2, 7
MT-104-8	4, 8	
MT-104-9	1, 6	Positive 1
MT-104-10	1, 6	
MT-104-11	3, 7	
MT-104-13	6, 8	
MT-104-16	3, 4	

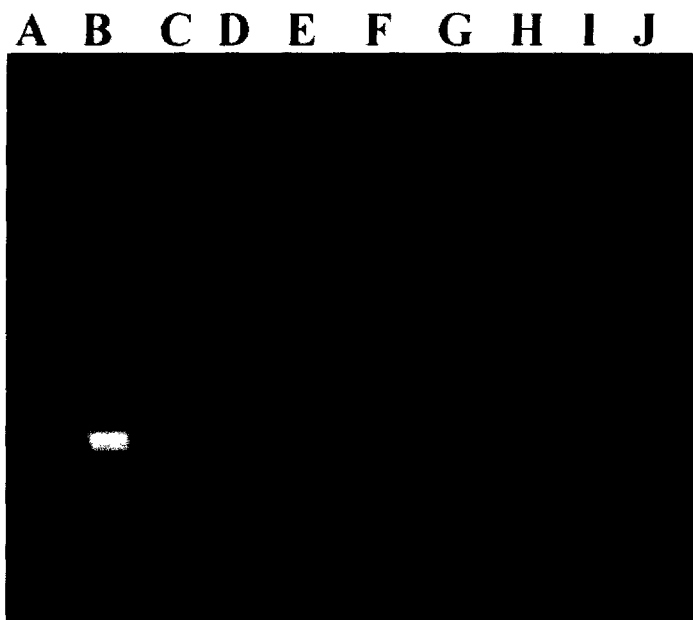


Figure 96. Gel electrophoresis of PCR products. Samples were prepared using the methods listed. Swabs were used to collect samples from individual pods from the new Medtronic Octopus 3[®] MT-104-1 and the reprocessed Medtronic Octopus 3[®] MT-104-3. DNA was extracted using the DNeasy DNA Extraction Kit, a single-copy 536 bp human β -globin fragment was amplified from each sample using standard PCR protocols, and the products were electrophoresed on a 10% polyacrlamide/TBE gel and stained with ethidium bromide (Molecular Probes). A) negative control, no PCR template, B) positive PCR control of 1 ng human genomic DNA template; C-F from new Medtronic Octopus 3[®], C) pod 1, D) pod 3, E) pod 5, F) pod 7; G-J from reprocessed Medtronic Octopus 3[®], G) pod 7, H) pod 5, I) pod 3, J) pod 1. **Pods 5 and 7 of the reprocessed Medtronic Octopus 3[®] are positive for human β -globin fragment.**

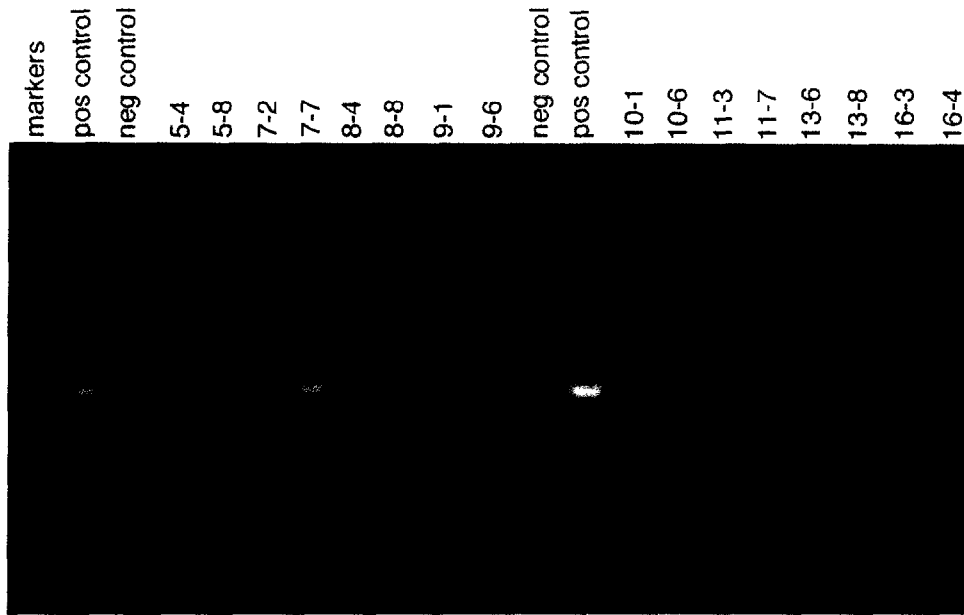


Figure 97. Samples were prepared using the methods listed. Swabs were used to collect material from two individual pods from each of the reprocessed devices. DNA was extracted using the Qiagen DNeasy[®] DNA Extraction Kit, a single-copy 536 bp human β -globin fragment was amplified from each sample using standard PCR protocols, and the products were electrophoresed on a 10% polyacrlamide/TBE gel and stained with ethidium bromide (Molecular Probes). Lanes are labeled as to contents. In numbered lanes, the first label number refers to the device ID and the second is the pod number (i.e. 5-4 is from MT-104-5, pod #4). Positive controls are PCR products of 1 ng human genomic DNA template; negative controls contain no PCR template. **Devices MT-104-7 and MT-104-9 are positive for human β -globin fragment.** Low intensity of the bands is likely due to the condition of the DNA and the small sample size (>1ng).

Disassembly and Cutting of Hypotubes

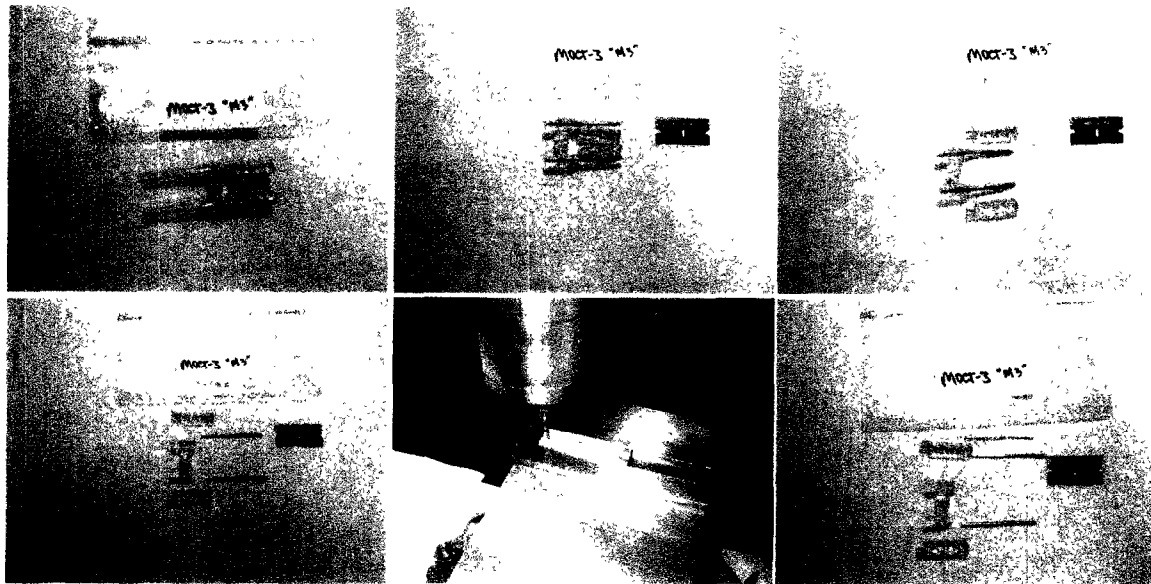


Figure 98. Series of images outlining the steps of hypotube removal and machining from the new Octopus3[®] MT-104-1.

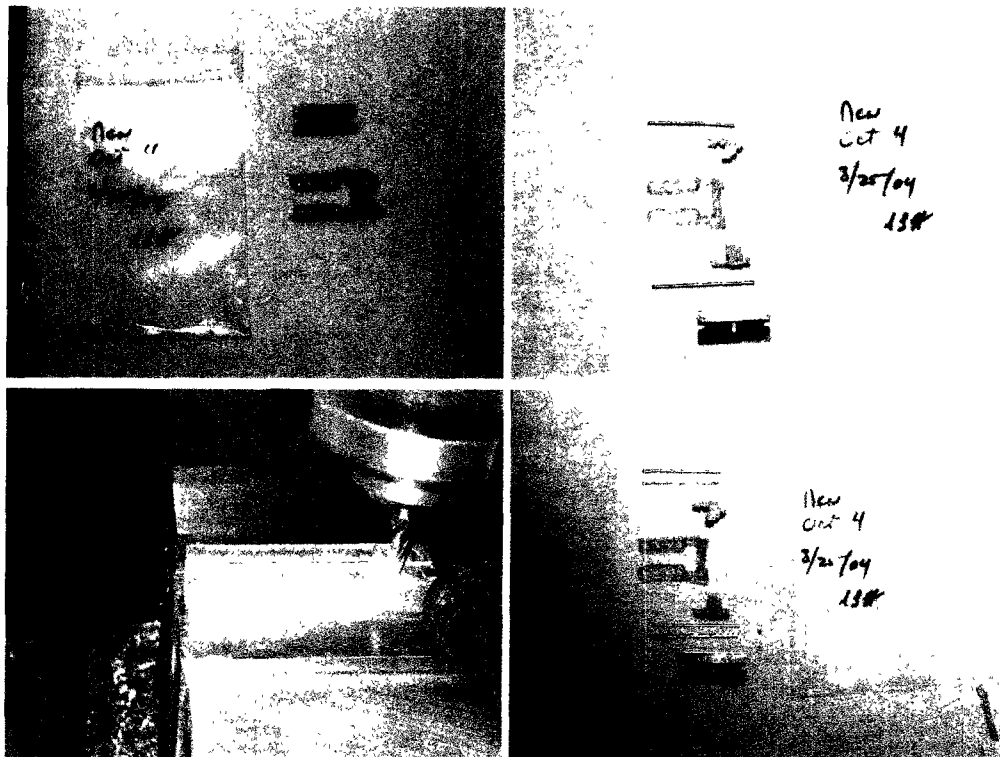


Figure 99. Series of images outlining the steps of hypotube removal and machining from the new Octopus4[®] MT-104-2.

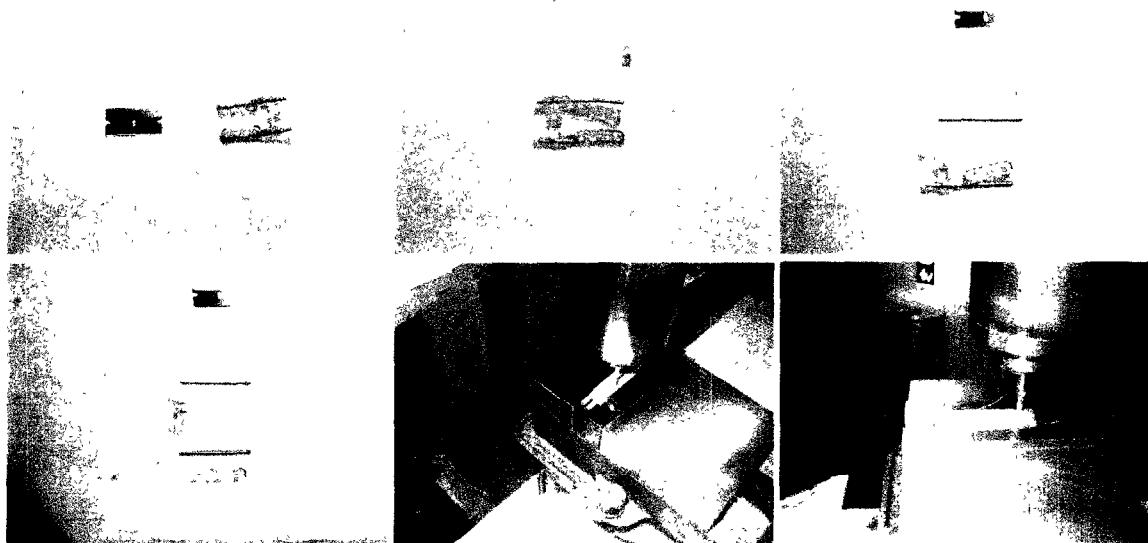


Figure 100. Series of images outlining the steps of hypotube machining and removal from the reprocessed Octopus3[®] MT-104-3.

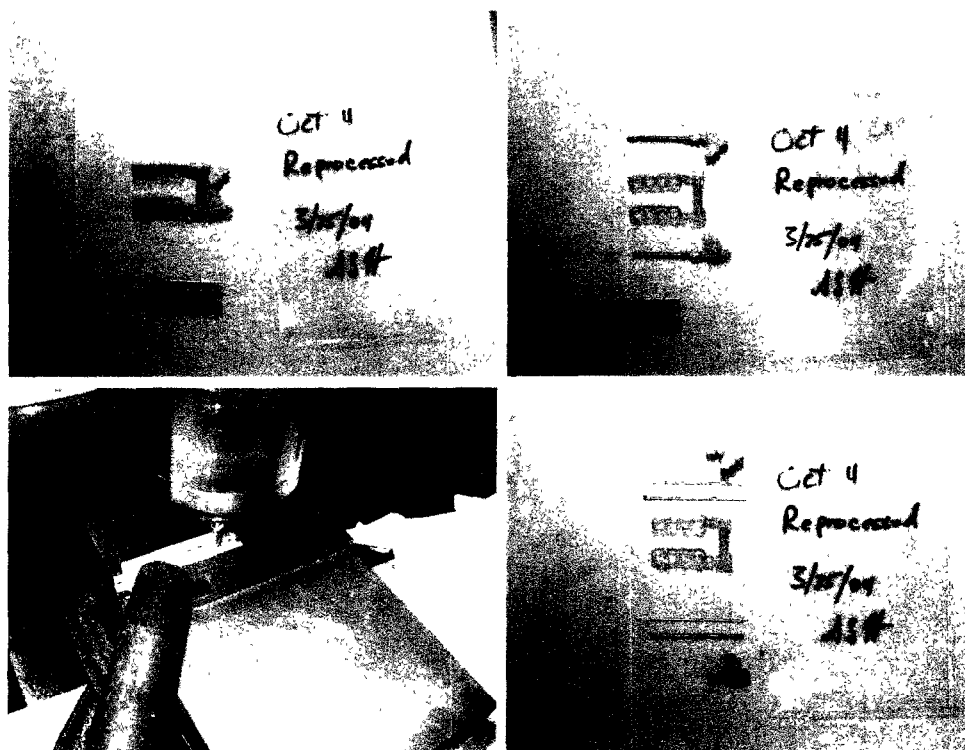


Figure 101. Series of images outlining the steps of hypotube removal and machining from the reprocessed Octopus4[®] MT-104-4.

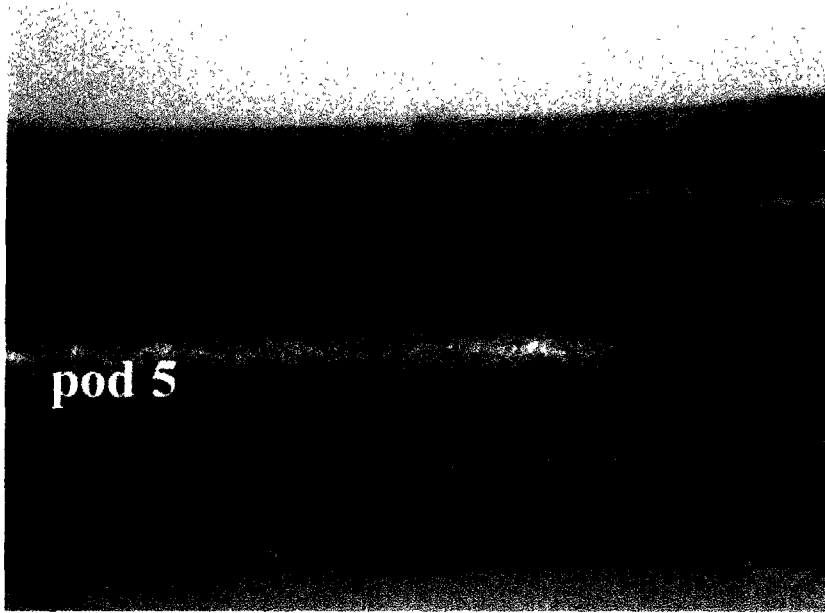


Figure 102. Image of the exposed interior end of the hypotube of the **reprocessed Octopus3[®] MT-104-3**. Note debris in hypotube opening (reddish tint from DNA staining procedure) and in dead end of the hypotube (indicated by arrow).

Scanning Electron Microscopy of Disassembled Hypotubes

Devices MT-104-1, 2, 3, 4 and 7 were selected for disassembly and cutting of the hypotube to expose the interior for further microscopic evaluations. The following images are of the interior of the hypotubes from those devices.

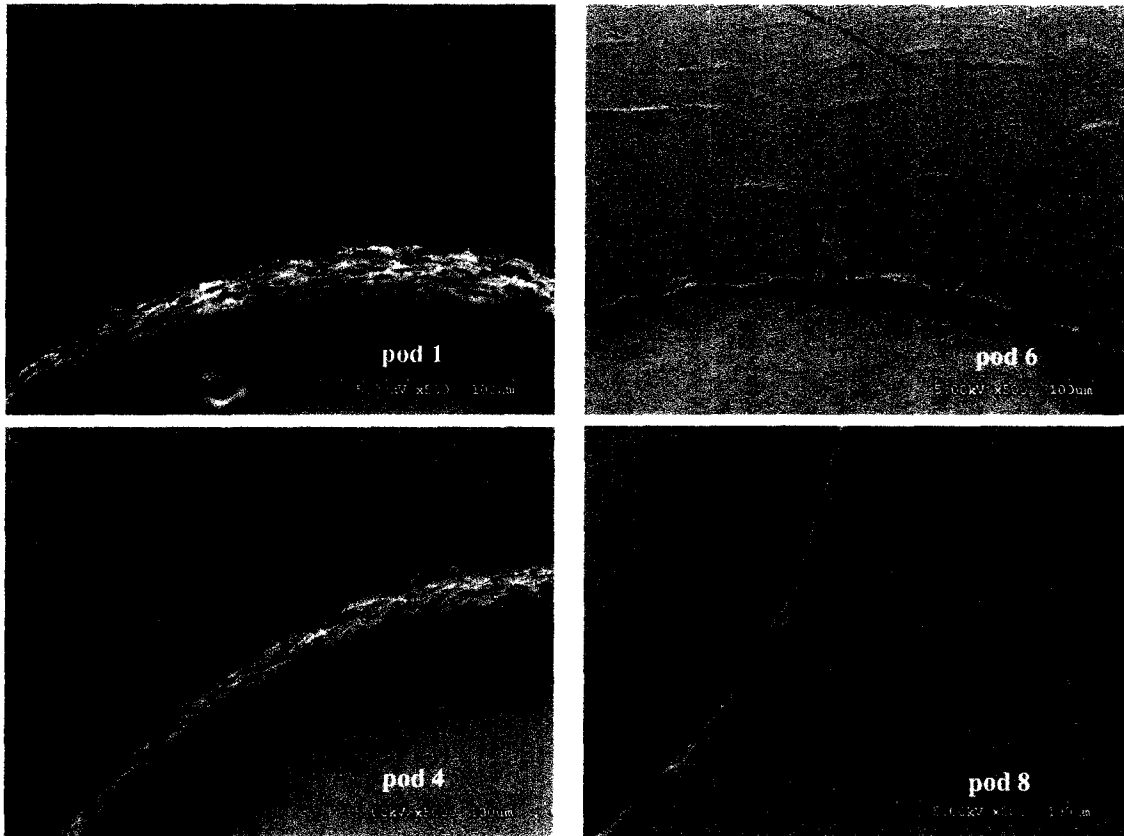


Figure 103. Series of images collected from Hitachi S3500N variable pressure scanning electron microscope of the inner surfaces following cutting in the areas of the orifices in the hypotube on the **new Octopus3[®] MT-104-1**. The images show relatively uniform surface structure on the metal surface of the tubing. The openings appear to be uniform in size and composition. There are what appear to be small pieces of debris in some wells. The debris does not appear organic. The label indicates the pod # (see Figure 5). Scale bar in each image.

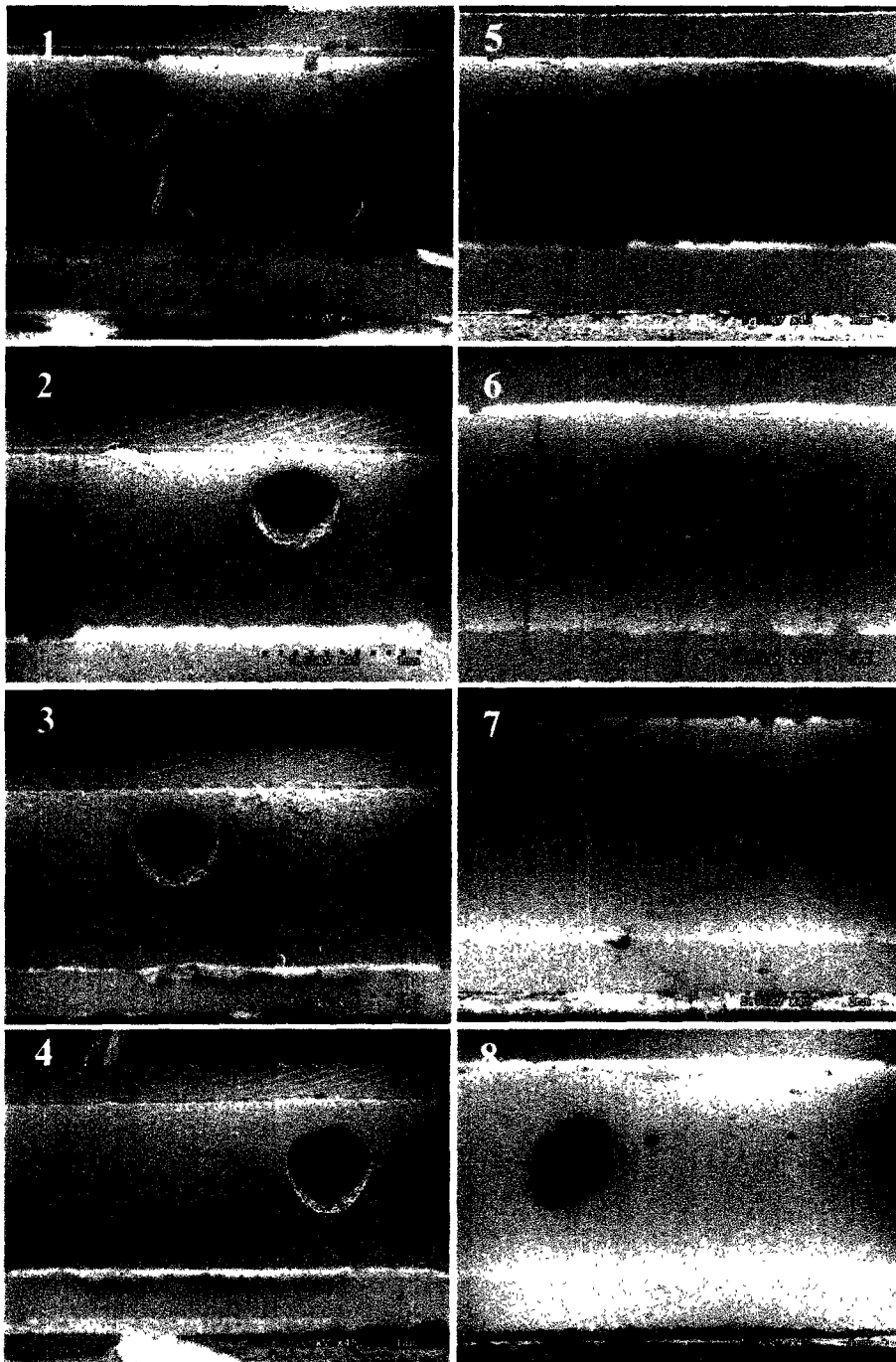


Figure 104. Series of images collected from Hitachi S3500N variable pressure scanning electron microscope of the inner surfaces of the tubing within the pods on the **reprocessed Octopus3[®] MT-104-3** following cutting. The images show irregularities on the inner surface structure of the tubing (e.g. in all pod regions to varying degrees). There is debris and irregularities present in the orifices of the tubing (e.g. in #1, #3, #5, #6, #7 and #8). The orifices are not as uniform in shape when compared to the “new” Octopus 3[®]. The numbers indicate the pod # (see Figure 5). This device has been imaged following staining for DNA. Scale bar in each image.

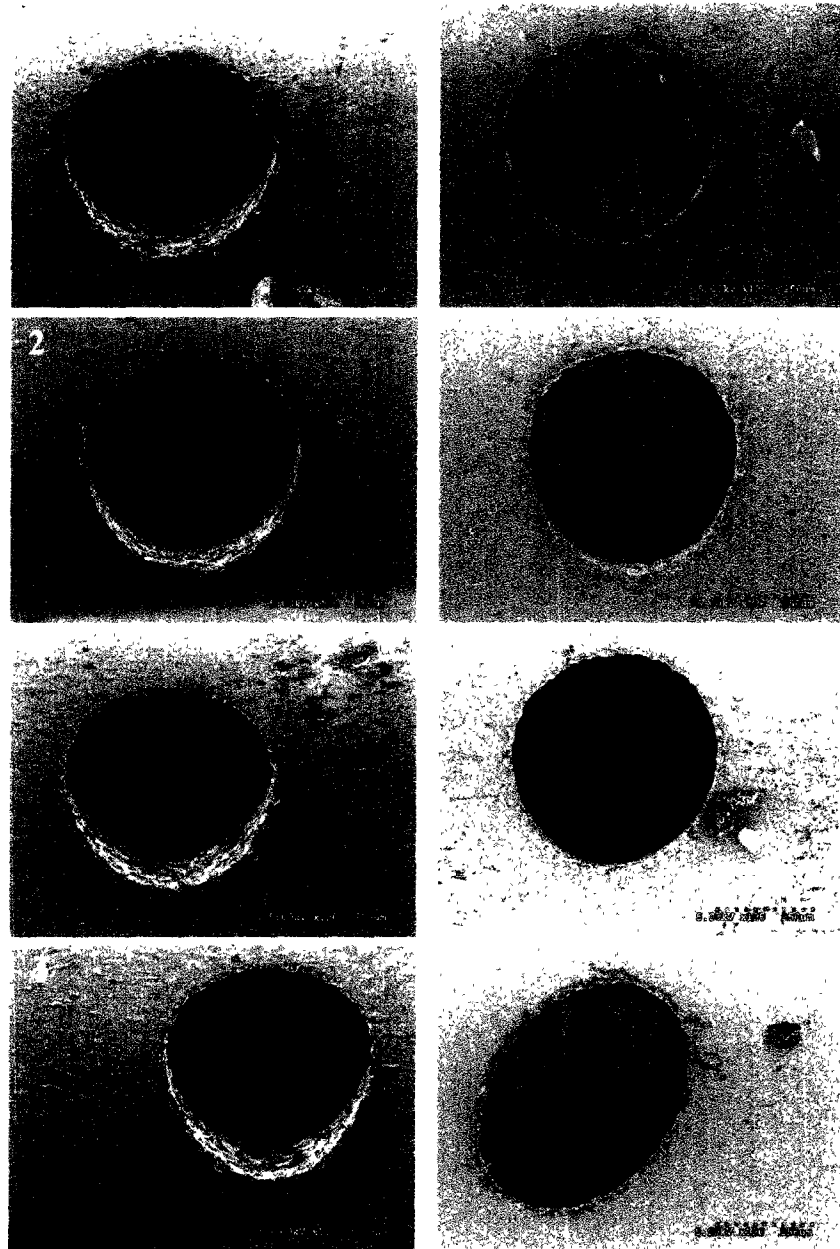


Figure 105. Series of images collected from Hitachi S3500N variable pressure scanning electron microscope of the inner surfaces of the tubing within the pods on the **reprocessed Octopus3[®] MT-104-3** following cutting. The images show irregularities on inner surface structure of the tubing (e.g. in all pod regions to varying degrees). There is debris, bioburden and irregularities present in the orifices of the tubing (e.g. in #1, #3, #5, #6, #7 and #8). The orifices are not as uniform in shape when compared to the “new” Octopus 3[®]. The numbers indicate the pod # (see Figure 5). This device has been imaged following staining for DNA. Scale bar in each image.

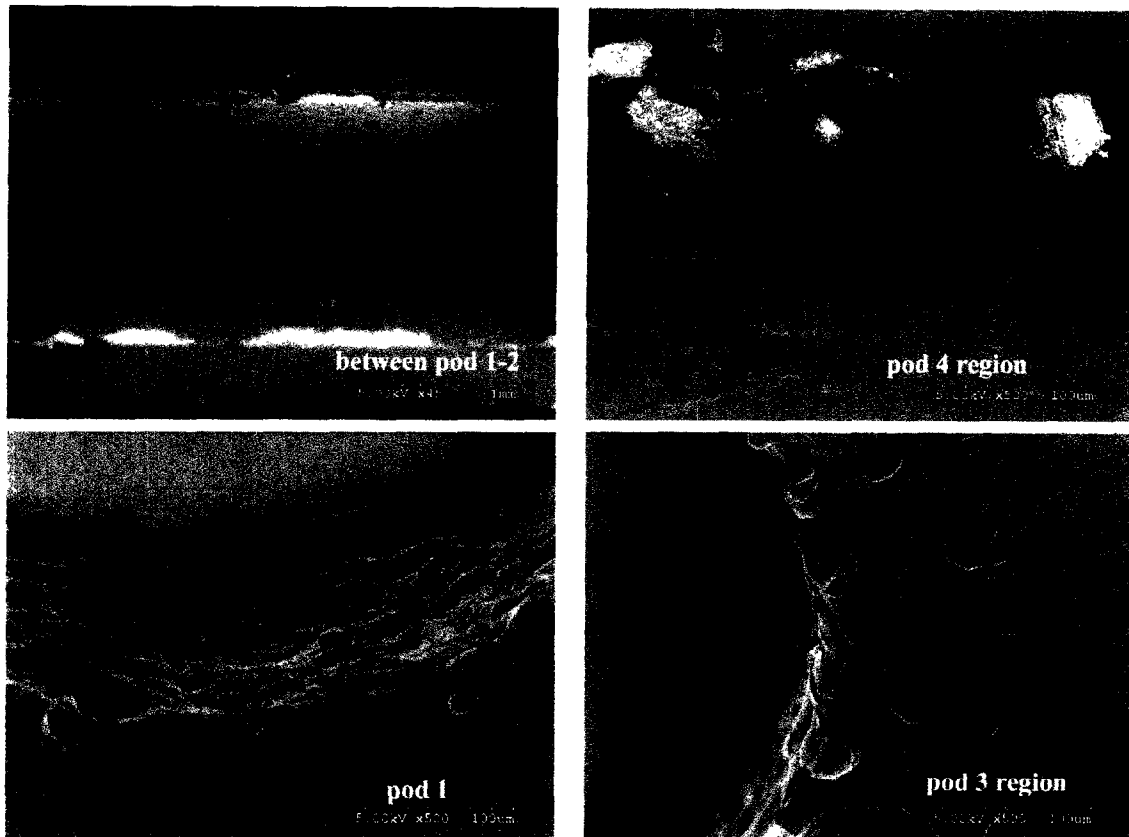


Figure 106. Series of images collected from Hitachi S3500N variable pressure scanning electron microscope of the tubing inner surface on the reprocessed Octopus3[®] MT-104-3. The images show irregularities to varying degrees on inner surface structure of the tubing in all regions. Bioburden and debris is present on the inner surface and in the orifices of the tubing. Note contaminating material coating the opening of the tubing orifice. Label indicates region imaged. Scale bar in each image.

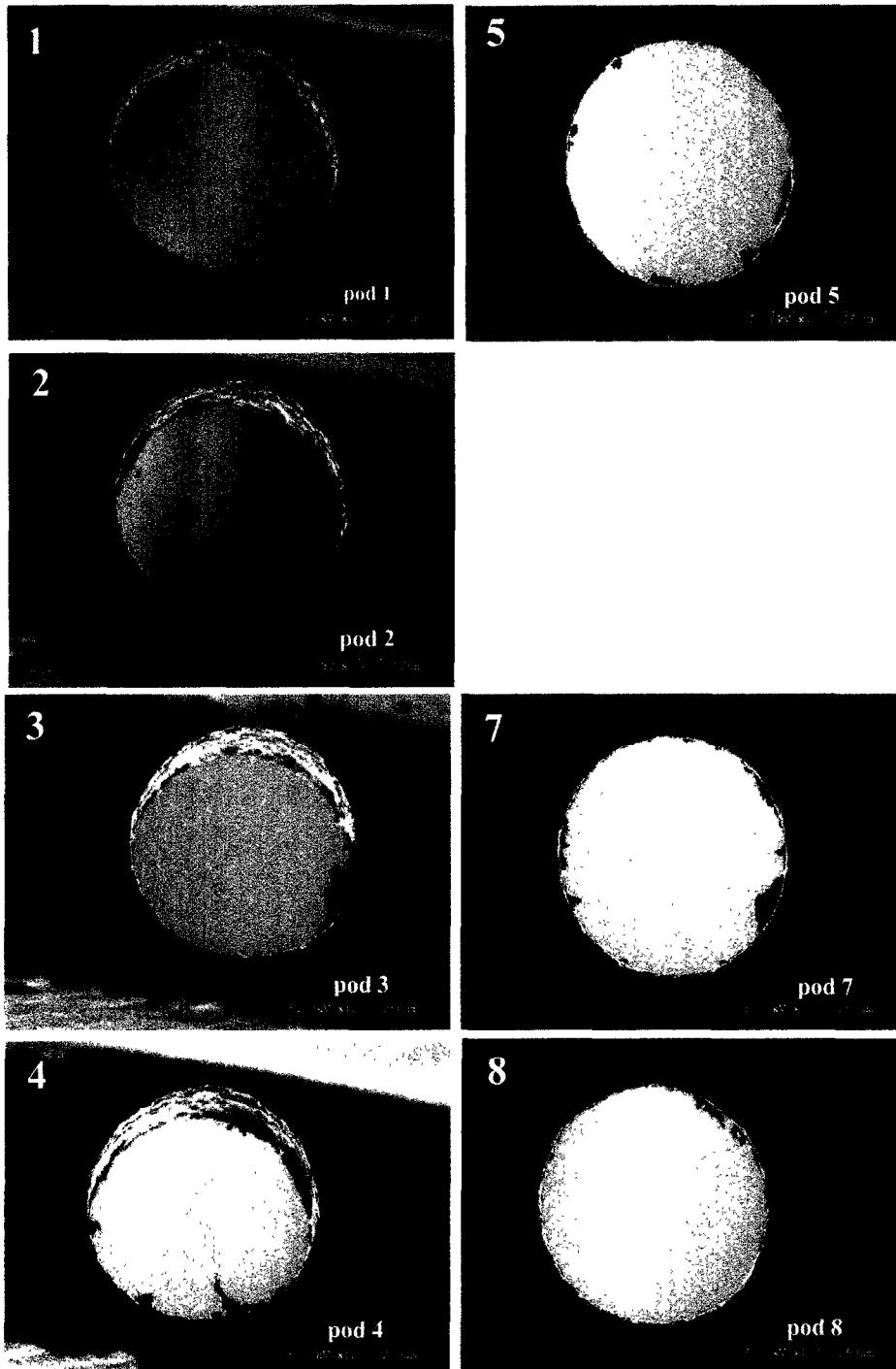


Figure 107. Series of images collected from Hitachi S3500N variable pressure scanning electron microscope of the inside surfaces of the tubing on the **new Octopus4[®] MT-104-2** following cutting. The images show uniform inner surface structure on the metal inner surface of the tubing. The openings appear to be uniform in size and composition. There are what appear to be small pieces of debris in some wells (e.g. #3, #7 and #8). The debris does not appear prior to disassembly and cutting of the device. The numbers indicate the pod # (see Figure 5). Scale bar in each image.

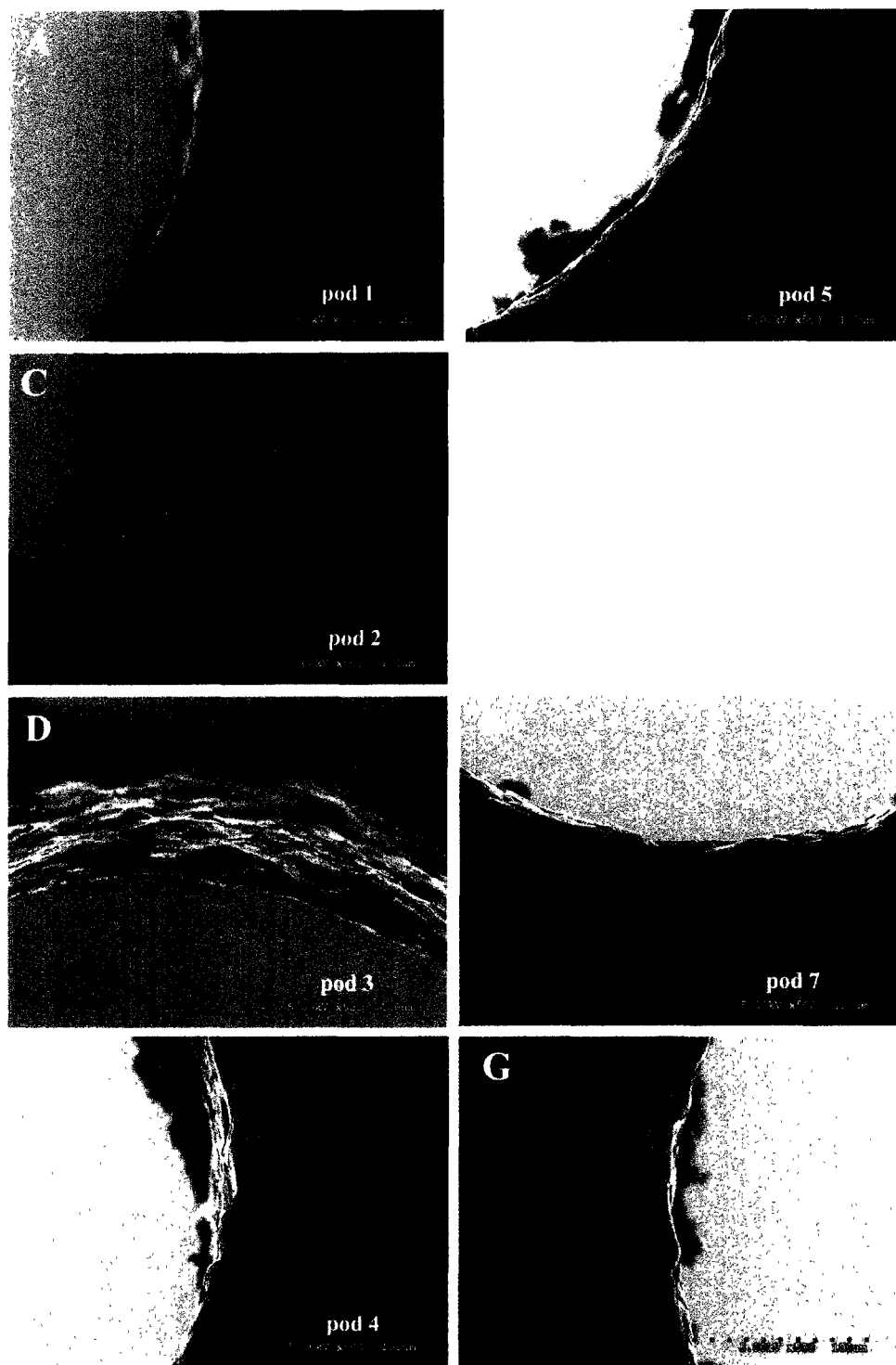


Figure 108. Series of images collected from Hitachi S3500N variable pressure scanning electron microscope in the areas of the orifices in the tubing within each pod on the **new Octopus4[®] MT-104-2**. The images show uniform inner surface structure on the metal of the tubing. The openings appear to be uniform in size and composition. There are what appear to be small pieces of debris in some openings (e.g. #3, #7 and #8). The debris does not appear organic. The numbers indicate the pod # (see Figure 5). Scale bar in each image.

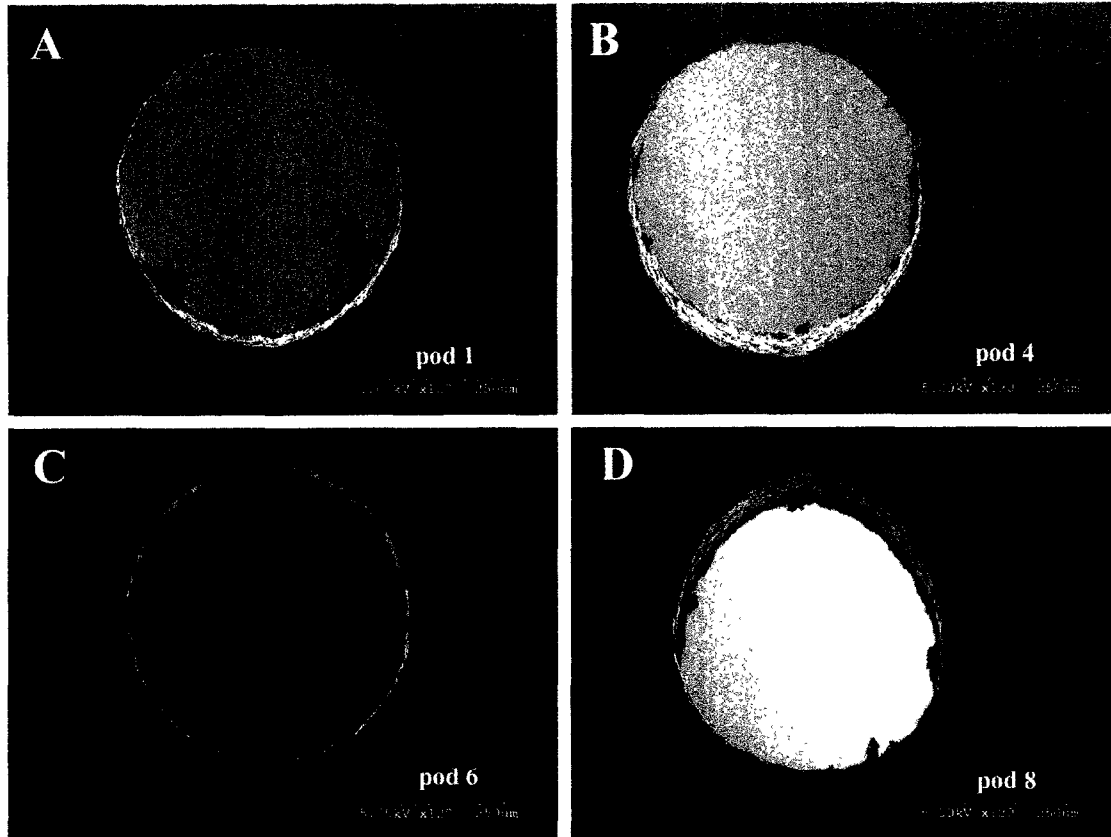


Figure 109. Series of images collected from Hitachi S3500N variable pressure scanning electron microscope in the areas of the orifices in the tubing within each pod on the **reprocessed Octopus4[®] MT-104-4**. The images show uniform surface structure on the metal surface of the tubing. The openings appear to be uniform in size and composition. There are what appear to be small pieces of debris in some wells (e.g. #3, #7 and #8). The debris does not appear organic. The numbers indicate the pod # (see Figure 5). Scale bar in each image.

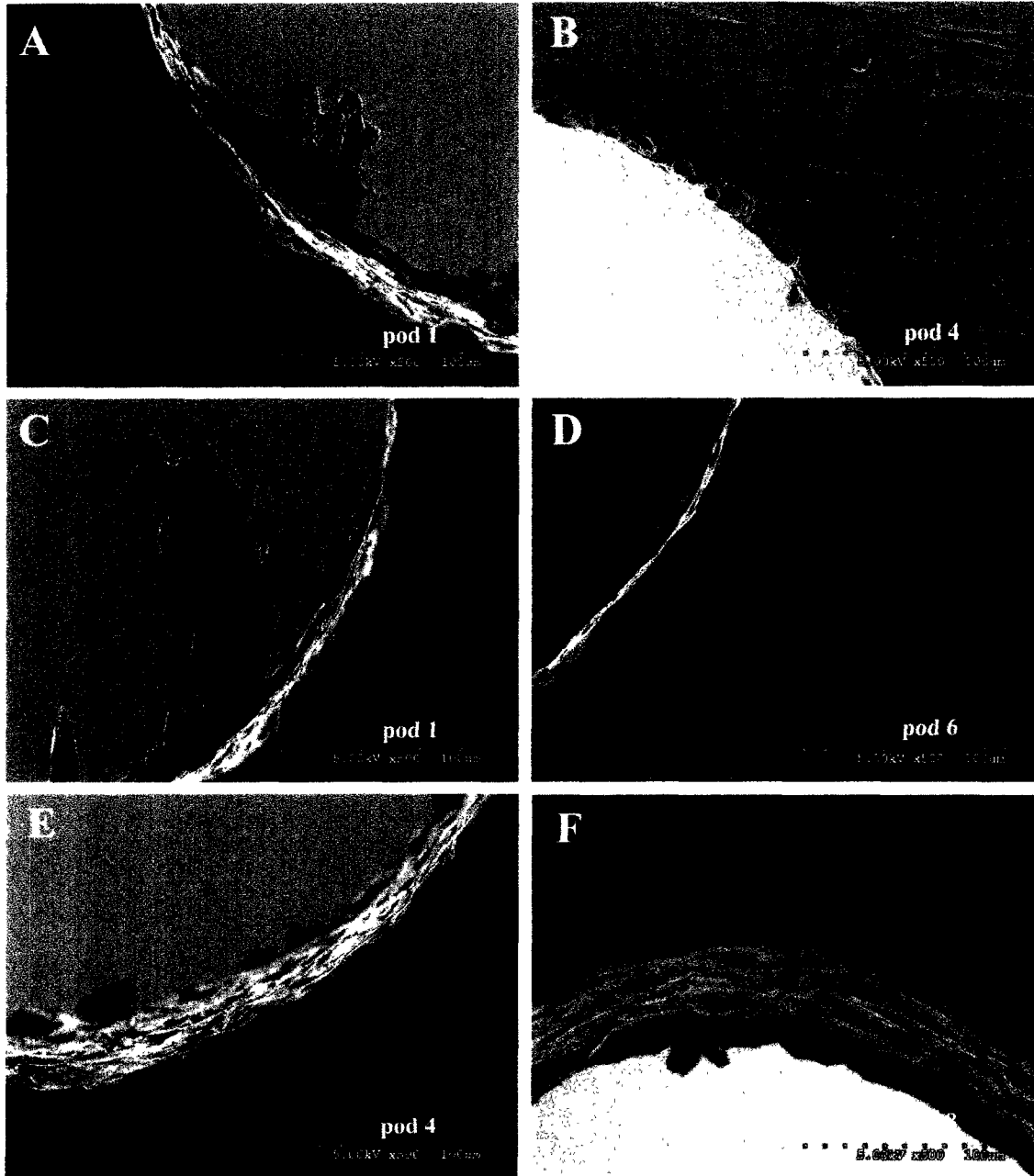


Figure 110. Series of images collected from Hitachi S3500N variable pressure scanning electron microscope in the areas of the orifices in the tubing within each pod on the **reprocessed Octopus4[®] MT-104-4**. The images show uniform surface structure on the metal surface of the tubing. The openings appear to be uniform in size and composition. There are what appear to be small pieces of debris in some wells (e.g. #3, #7 and #8). The debris does not appear organic. The numbers indicate the pod # (see Figure 5). Scale bar in each image.

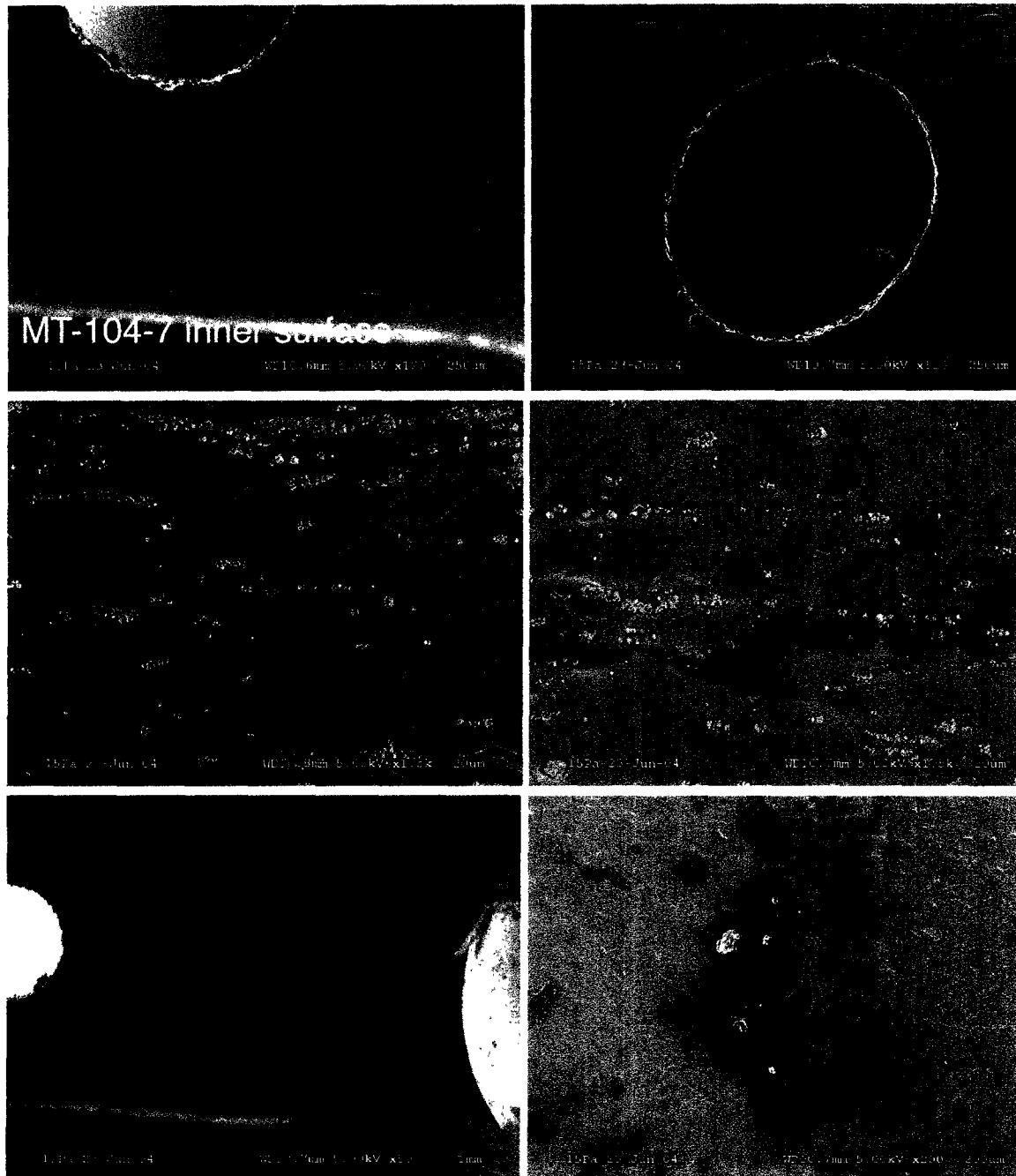


Figure 111. Series of images collected from Hitachi S3500N variable pressure scanning electron microscope in areas inside the hypotubing on the **reprocessed Octopus3[®] MT-104-7**. The images show irregularities and contamination to varying degrees on inner surface structure of the tubing in various regions. Bioburden and debris is present on the inner surface and in the orifices of the tubing. Scale bar in each image.

CONCLUSIONS

Our studies have shown there is no sign of usage, little to no debris on the new Medtronic Octopus 3[®] or the Medtronic Octopus 4[®] head region when observed by light and scanning electron microscopes and DNA analysis. The debris present appeared to be microscopic, non-organic and typical of the manufacturing process.

Although there is variability in the amount and severity of contamination and defects between the reprocessed devices supplied for this study, the results of the light microscopy and scanning electron microscopy, protein and DNA testing clearly demonstrate the presence of artifacts, defects and biological contamination including corrosion of surfaces, dried salts, foreign debris, fibers, human hair, protein and nucleic acid positive material on the headlink and ball joint regions of the reprocessed Octopus[®] Tissue Stabilizers when compared to a new, sterile device. Two head links have physical defects that either partially or completely block the openings of the hypotubes that would likely affect their performance. There is corrosion and debris present in the ball joint region of the flexible arm particularly in devices MT-104-3, 5, 7, 8 and 9. The positive reaction of the bioburden with the nucleic acid specific stains propidium iodide and Syto 16 confirm the presence of nucleic acids associated with the much of the material in the vast majority of the reprocessed Octopus 3[®] and Octopus 4[®] devices. The positive reaction of the bioburden with the protein specific stain Sypro[®] Orange confirm the presence of protein associated with the much of the material in the vast majority of the reprocessed Octopus 3[®] and Octopus 4[®] devices (see Tables IV and V for summary). Similar material was also found in internal surfaces of the hypotubes of these reprocessed devices and is likely positive for these probes. Additional PCR based DNA testing confirm the presence of human β -globin fragment in the several pod regions of the reprocessed devices.

Taken together, these results bring into question the effectiveness of the reprocessing efforts.

Respectfully submitted,



Mark A. Sanders, Program Director
Imaging Center,
123 Snyder Hall
1447 Gortner Avenue
St. Paul, MN 55108-5754
ph: 612-624-3454

Table IV.

Summary table of new and reprocessed Octopus[®] devices

Device code ID	Normal -as new	Unknown Material Contamination	Bio-contamination (Syto 16 positive)	Bio-contamination (Sypro Orange positive)	Physical defect
MT-104-1	+	-	-	-	-
MT-104-2	+	-	-	-	-
MT-104-3	-	+	+		+
MT-104-4	+	-	-	-	-
MT-104-5	-	+	+	+	+
MT-104-7	-	+	+	+	+
MT-104-8	-	+	+	+	+
MT-104-9	-	+	+	+	+
MT-104-10	-	+	+	+	+
MT-104-11	-	+	+	+	-
MT-104-13	-	+	+	+	+
MT-104-16	-	+	+	+	-

Table V.
Summary table of pods affected in reprocessed Octopus[®] devices

Device code ID	# of pods Normal –as new ((#) indicates pod #)	# of pods Material contamination	# of pods DNA contamination (PI/Syto 16 positive)	# of pods Protein contamination (Sypro Orange positive)	# of pods Physical defect
MT-104-1	(8) 12346578				
MT-104-2	(8) 12346578				
MT-104-3		(8) 12346578	(4) 357		
MT-104-4	(8) 12346578				
MT-104-5		(8) 12346578	(3) 125	(3) 357	(2) 46
MT-104-7		(8) 12345678	(4) 1235		(2) 28
MT-104-8		(8) 12345678	(3) 467	(3) 357	(1) 8
MT-104-9		(8) 12345678	(6) 125678	(3) 458	(2) 78
MT-104-10		(8) 12345678	(5) 34578		(2) 45
MT-104-11		(8) 12345678	(4) 1268		
MT-104-13		(8) 12345678	(2) 17	(2) 37	(4) 1234
MT-104-16		(8) 12345678	(5) 34678		

List of physical defects (by device)

MT-104-3

Pod 4 – irregular shaped hypotube opening
Pod 5 – irregular shaped hypotube opening
Pod 7 – irregular shaped hypotube opening
Pod 8 – irregular shaped hypotube opening

MT104-5

Pod 4 – irregular shaped hypotube opening
Pod 6 – tear in plastic

MT104-7

Pod 2 – irregular shaped hypotube opening
Pod 8 – irregular shaped hypotube opening

MT104-8

Pod 8 – irregular shaped hypotube opening

MT104-9

Pod 7 – scratch in hypotube
Pod 8 – scratch in hypotube

MT104-10

Pod 4 – partially blocked hypotube opening
Pod 5 – scratches on hypotube

MT104-13

Pod 1 – partially blocked hypotube opening
Pod 2 – partially blocked hypotube opening
Pod 3 – partially blocked hypotube opening
Pod 4 – totally blocked hypotube opening